Supplementary information for: Constraints on the upper mantle structure beneath the Pacific from 3-D anisotropic waveform modelling

E. Kendall [1], A.M.G. Ferreira [1,2], S.-J. Chang [3], D. Peter [4]

[1] Department of Earth Sciences, University College London, London, UK 2 CERIS, Instituto Superior Técnico, Universidade de Lisboa, Lisbon, Portugal 3 Division of Geology and Geophysics, Kangwon National University, Chuncheon, South Korea 4 Extreme Computing Research Center, King Abdullah University of Science and Technology (KAUST), Thuwal, Saudi Arabia

Contents of this file

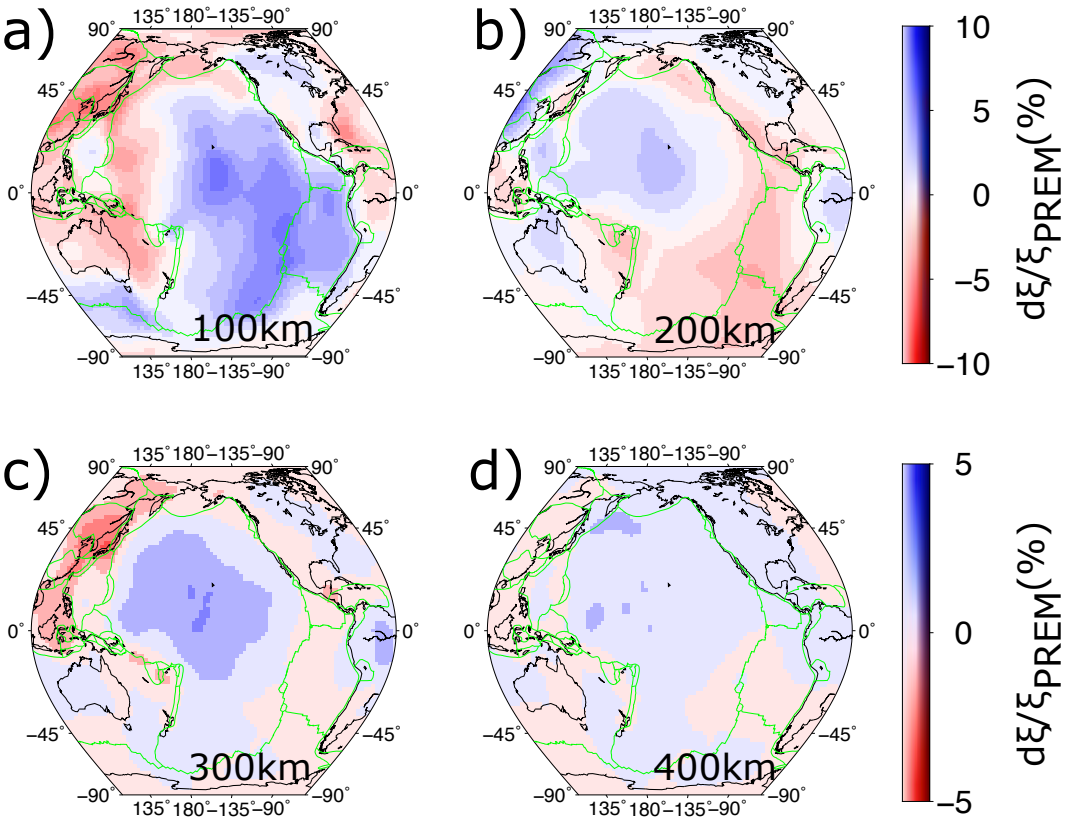

Figure S1. Perturbations with respect to PREM in the radially anisotropic ξ structure of SGLOBE-smooth at a) 100 km, b) 200 km, c) 300 km and d) 400 km depth.

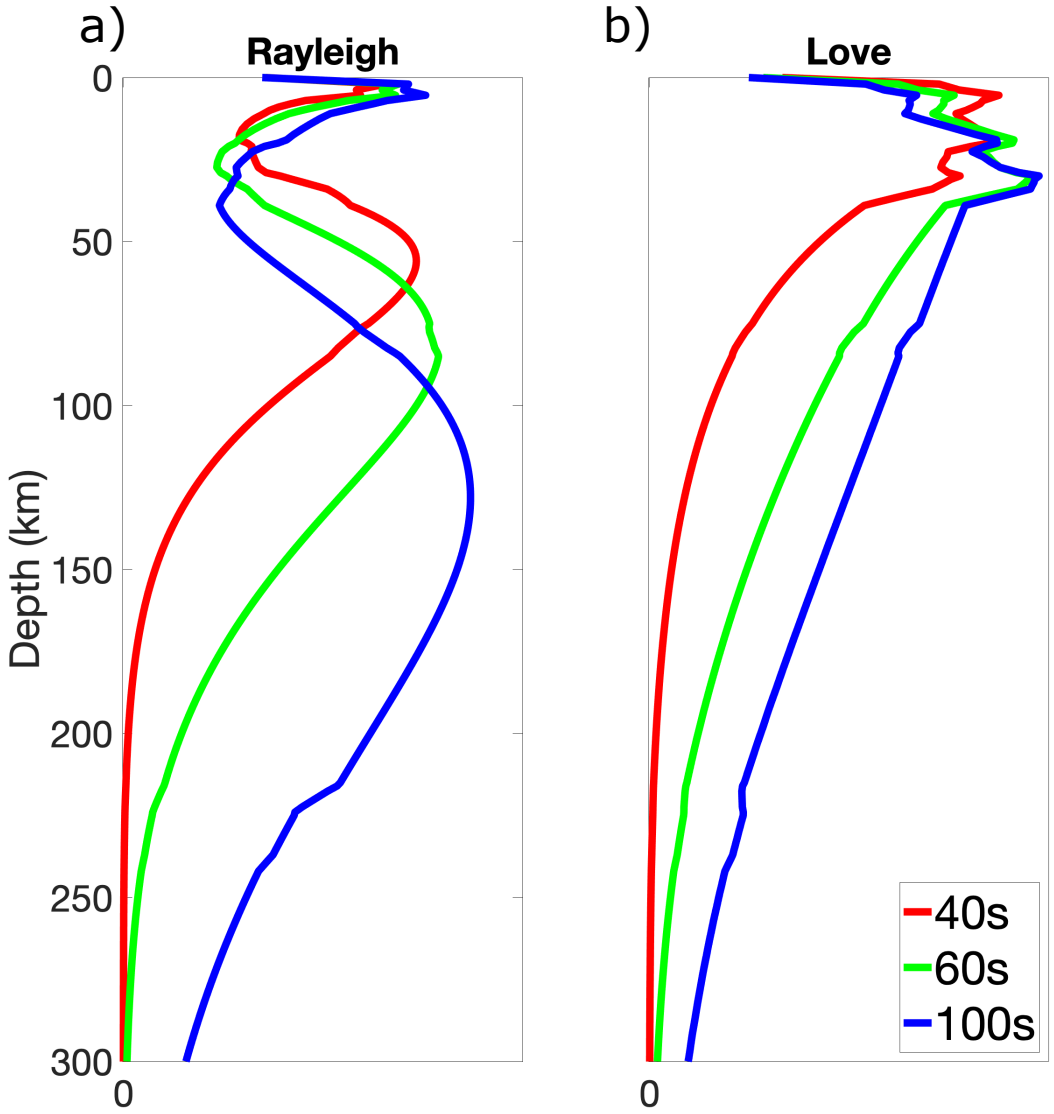

Figure S2. Normalized a) Rayleigh and b) Love wave fundamental mode phase-velocity kernels with respect to the vertically polarized ($\frac{dC}{dV_{SV}}$) and horizontally polarized shear wave ($\frac{dC}{dV_{SH}}$), respectively at wave periods of T∼40 s (red), 60 s (green) and 100 s (blue). The 1D reference model PREM is used to compute the kernels.

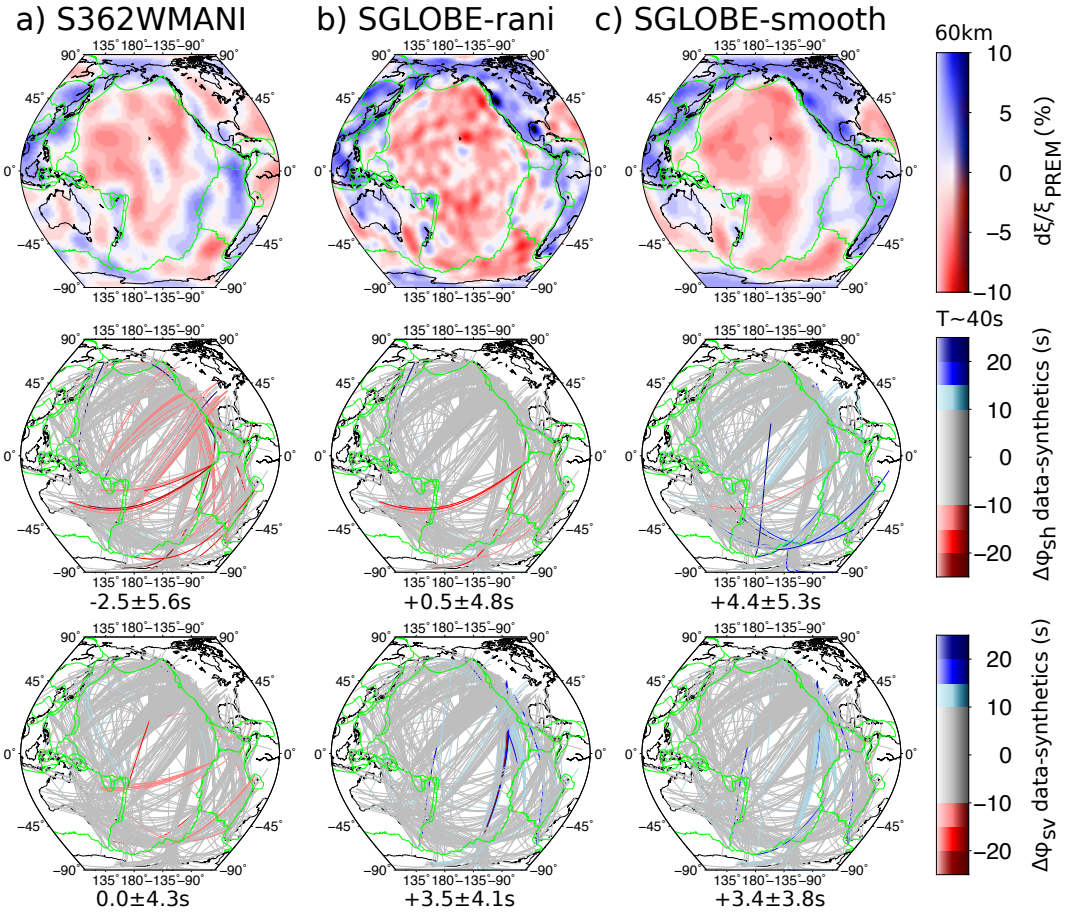

Figure S3. Top row: depth slices of perturbations in radially anisotropic anomalies with respect to PREM at 60 km depth in the Pacific for a) S362WMANI, b) SGLOBE-rani and c) SGLOBE-smooth. Fundamental mode Love (middle row) and Rayleigh (bottom row) wave phase misfits for waveforms filtered with a dominant wave period of T∼40 s, color-coded for synthetics fitting the data within 10 s (grey), more than 10 s slower than the data (pink-brown), more than 10 s faster than the data (blue). The median and standard deviation for each model are shown at the bottom of each subplot.

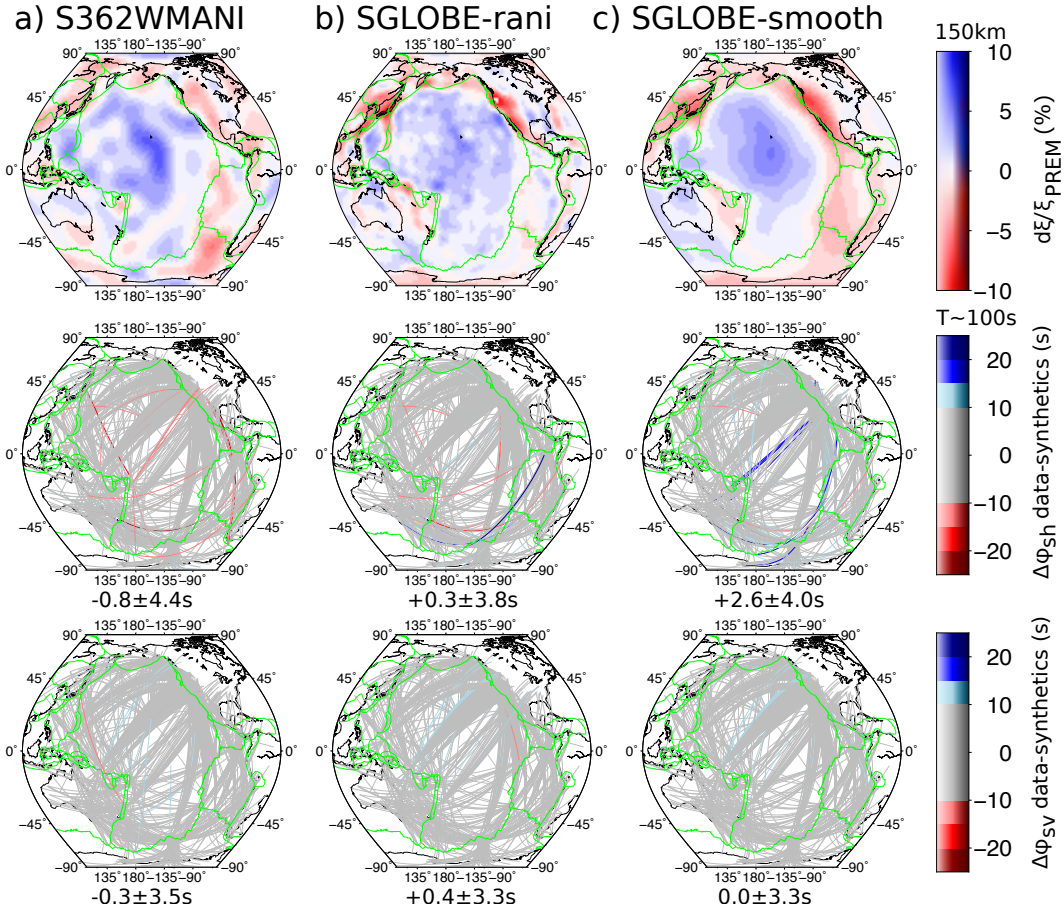

Figure S4. Top row: depth slices of perturbations in radially anisotropic anomalies with respect to PREM at 150 km depth in the Pacific for a) S362WMANI, b) SGLOBE-rani and c) SGLOBE-smooth. Fundamental mode Love (middle row) and Rayleigh (bottom row) wave phase misfits for waveforms filtered with a dominant wave period of T∼100 s, color-coded for synthetics fitting the data within 10 s (grey), more than 10 s slower than the data (pink-brown), more than 10 s faster than the data (blue). The median and standard deviation for each model are shown at the bottom of each subplot.

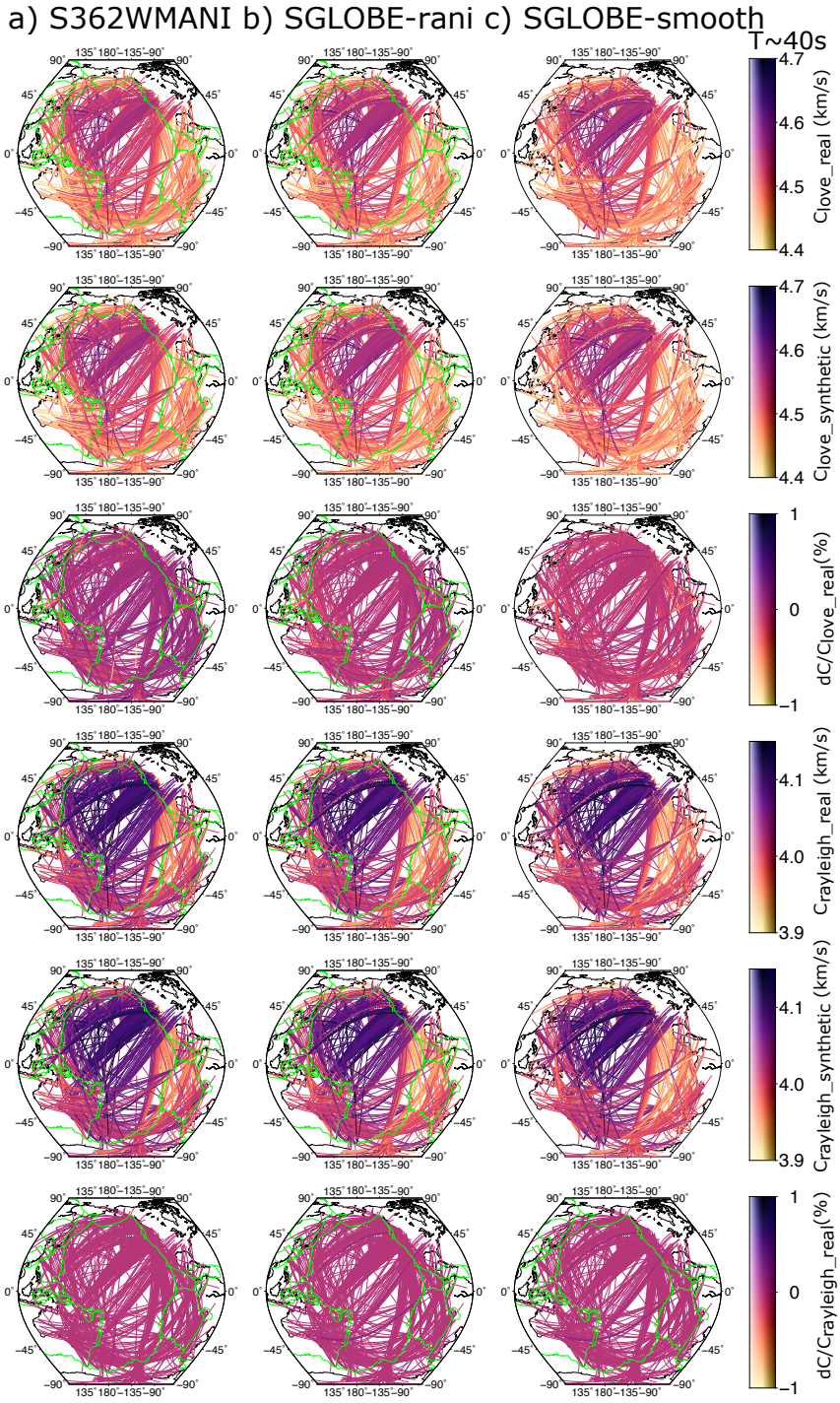

Figure S5. Geographical distribution of real (first row), modified synthetic (second row) Love wave phase velocities and the percentual difference between them (third row) at T∼40 s for a) S362WMANI, b) SGLOBE-rani and c) SGLOBE-smooth. The same format is shown for Rayleigh wave phase velocities (fourth to sixth rows). The percentual differences shown in the third and sixth rows are mostly lower than 0.1%, which shows that our associated estimates of Earth structure lead to a good fit to the data.

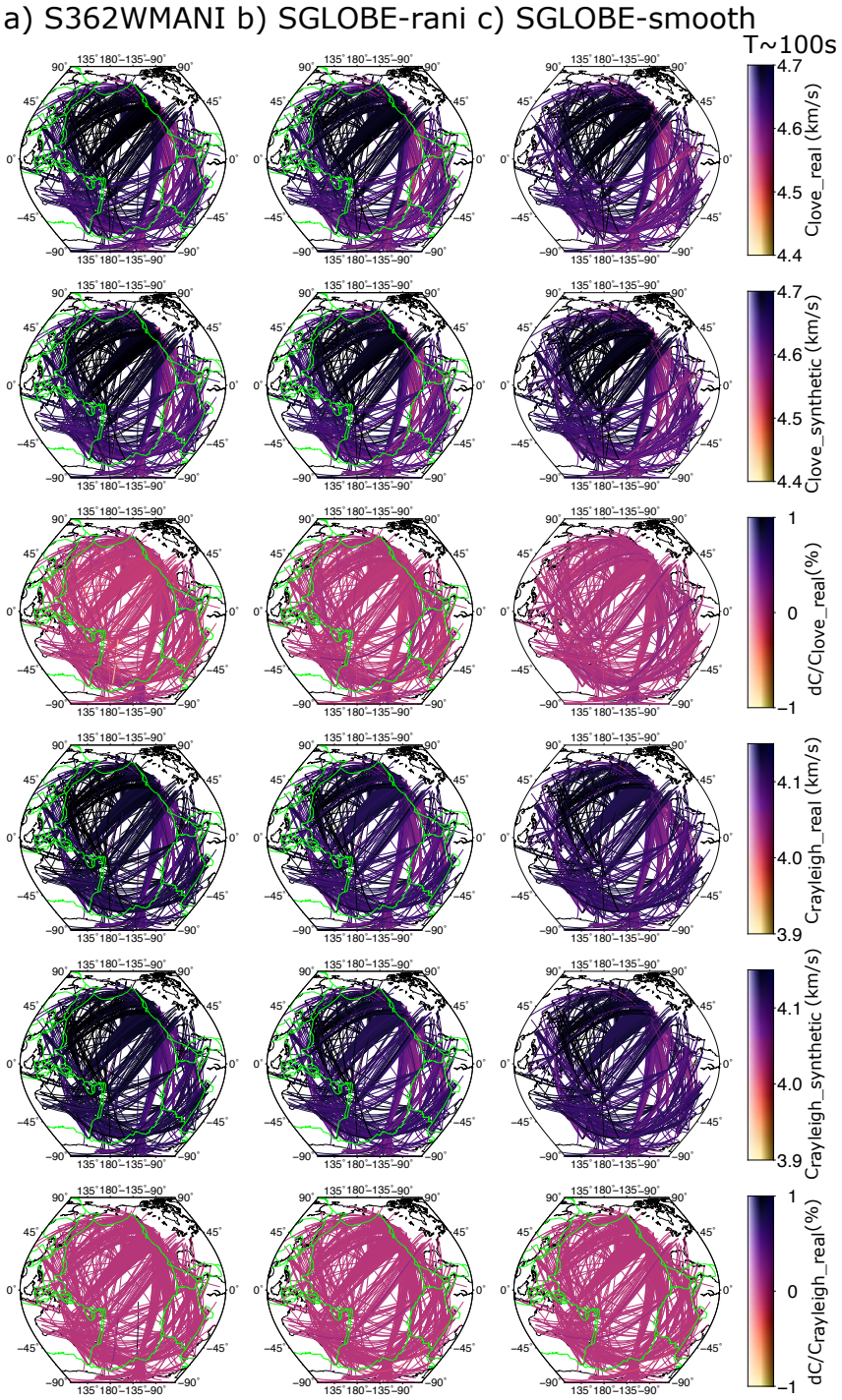

Figure S6. Geographical distribution of real (first row), modified synthetic (second row) Love wave phase velocities and the percentual difference between them (third row) at T∼100 s for a) S362WMANI, b) SGLOBE-rani and c) SGLOBE-smooth. The same format is shown for Rayleigh wave phase velocities (fourth to sixth rows). The percentual differences shown in the third and sixth rows are mostly lower than 0.1%, which shows that our associated estimates of Earth structure lead to a good fit to the data.

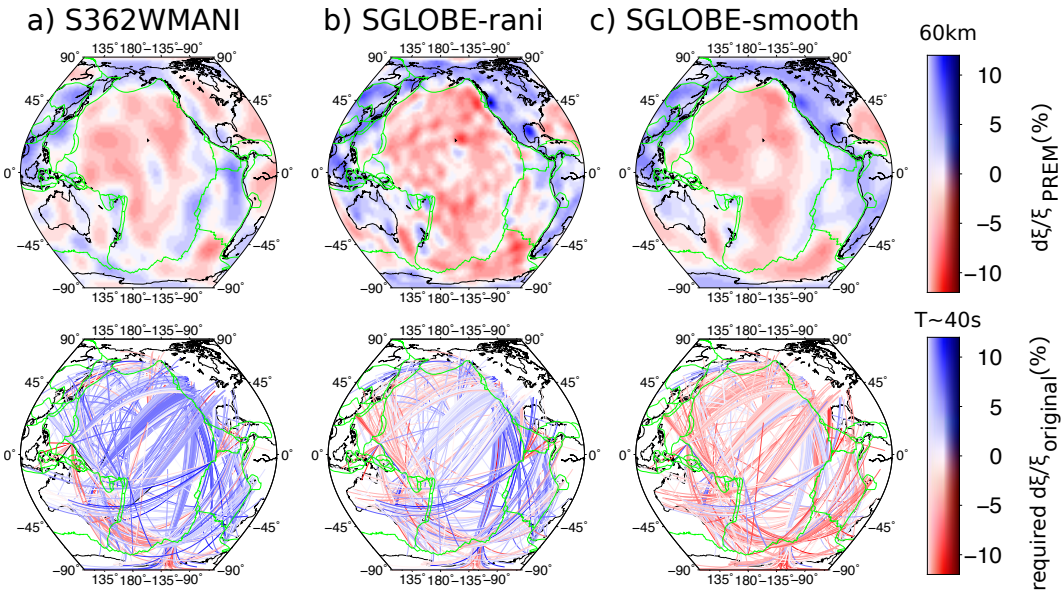

Figure S7. Depth slices of perturbations in radially anisotropic anomalies with respect to PREM at 60 km depth (top) in the Pacific for a) S362WMANI, b) SGLOBE-rani and c) SGLOBE-smooth. The geographical distribution of the required adjustments in radial anisotropy with respect to the original anisotropy are shown in the middle (bottom). Blue (red) colors indicate that positive (negative) anisotropic anomalies with respect to the original anisotropy are required to fit the data.

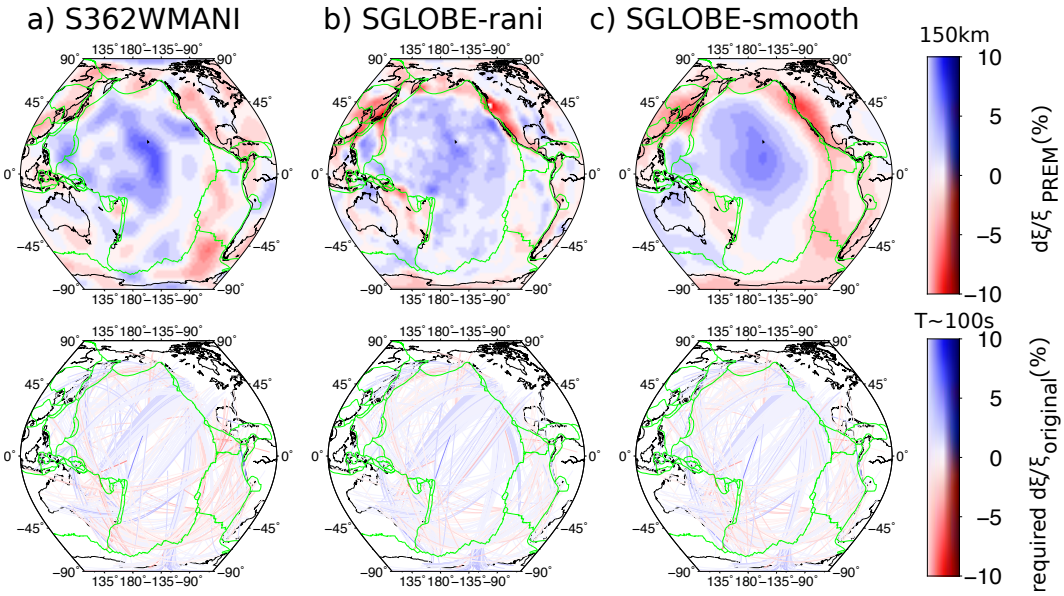

Figure S8. Depth slices of perturbations in radially anisotropic anomalies with respect to PREM at 150 km depth (top) in the Pacific for a) S362WMANI, b) SGLOBE-rani and c) SGLOBE-smooth. The geographical distribution of the required adjustments in radial anisotropy with respect to the original anisotropy are shown in the middle (bottom). Blue (red) colors indicate that positive (negative) anisotropic anomalies with respect to the original anisotropy are required to fit the data.

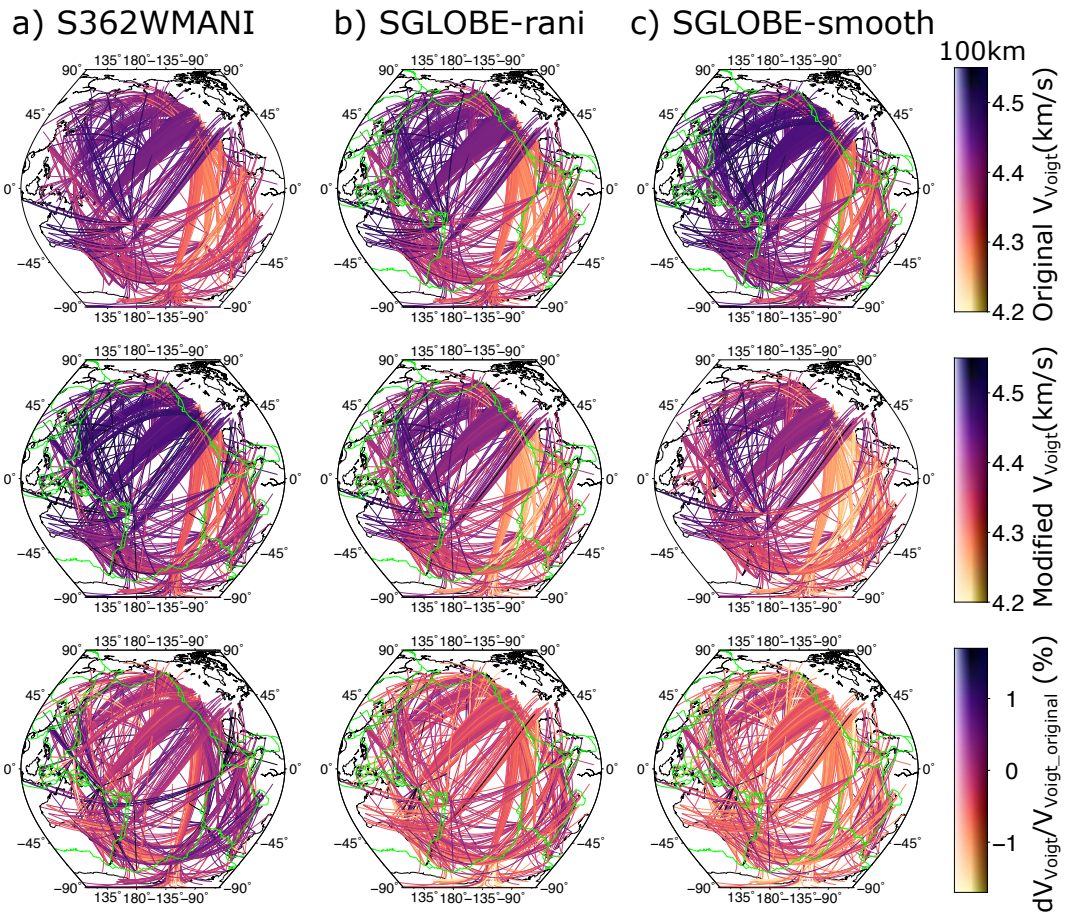

Figure S9. Original (top), modified (middle) and percentage difference between original and modified isotropic V_S structure (Voigt average, V_{Voigt}) (bottom) along path in a) S362WMANI, b) SGLOBE-rani and c) SGLOBE-smooth at ∼100 km depth.

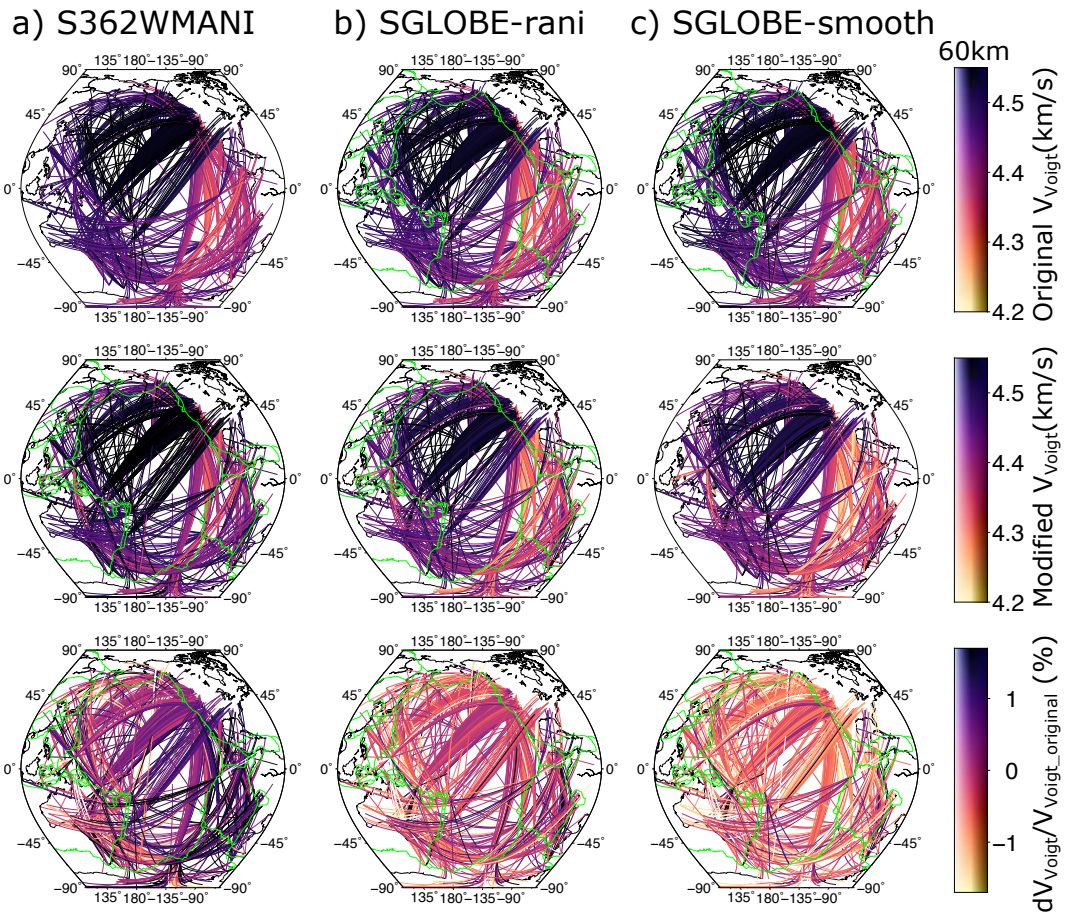

Figure S10. Original (top), modified (middle) and percentage difference between original and modified isotropic V_S structure (Voigt average, V_{Voigt}) (bottom) along path in a) S362WMANI, b) SGLOBE-rani and c) SGLOBE-smooth at ∼60 km depth.

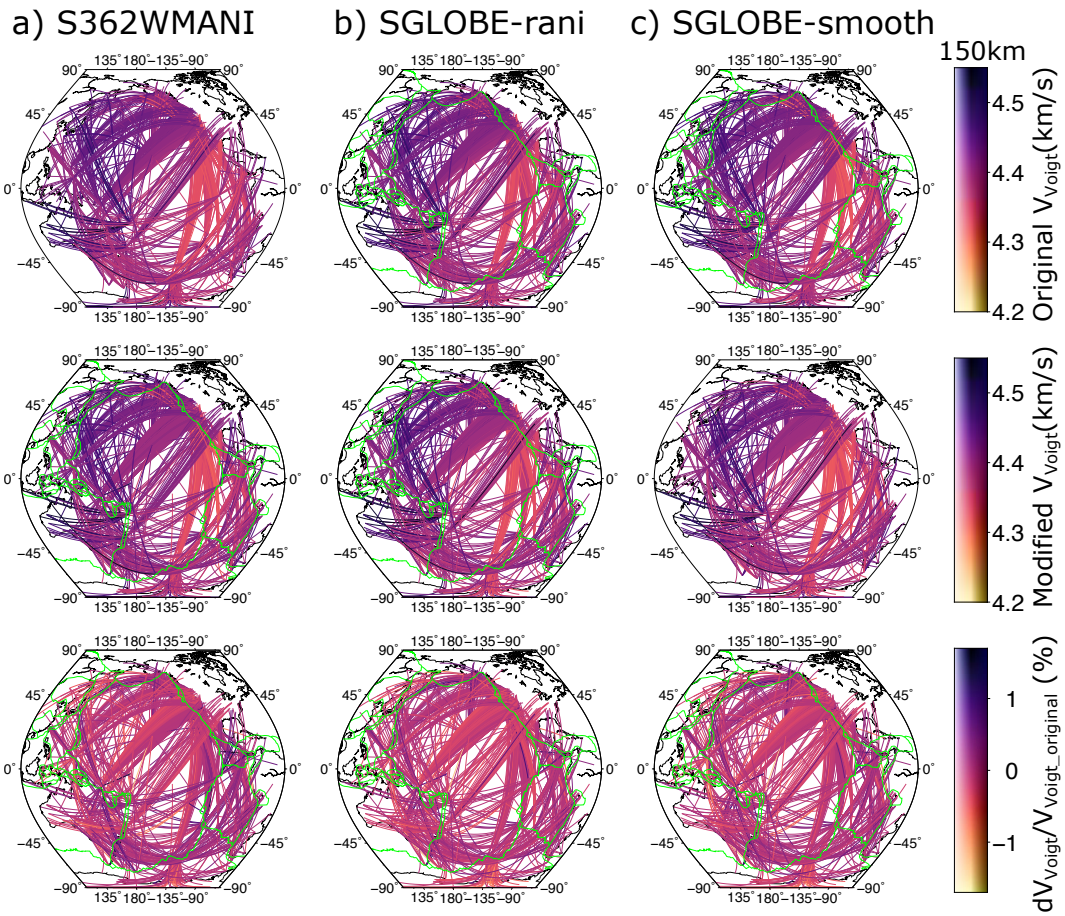

Figure S11. Original (top), modified (middle) and percentage difference between original and modified isotropic V_S structure (Voigt average, V_{Voigt}) (bottom) along path in a) S362WMANI, b) SGLOBE-rani and c) SGLOBE-smooth at ∼150 km depth.